

DOI 10.24425/ae.2022.142119

Design methods for limiting rotor losses in a fractional slot PMSM motor with high power density

TOMASZ WOLNIK  , SZCZEPAN OPACH , ŁUKASZ CYGANIK ,
TOMASZ JAREK , VOJTECH SZEKERES 

*Lukasiewicz Research Network – Institute of Electrical Drives and Machines KOMEL
Al. Roździeńskiego 188, 40-203 Katowice, Poland*

*e-mail: { tomasz.wolnik/szczepan.opach/lukasz.cyganik/tomasz.jarek}@komel.lukasiewicz.gov.pl,
vojtik21@gmail.com*

(Received: 07.06.2022, revised: 12.07.2022)

Abstract: Fractional slot PMSM motors enable high power density factors to be obtained provided that their electromagnetic circuit, appropriate mechanical structure and cooling system are properly designed, as well as when operating at a high frequency of power supply voltage (400–800 Hz) with high magnetic saturation and high current loads (approx. 12–15 A/mm²). Such operating conditions, especially in the case of fractional slot motors, may be the reason for excessive rotor losses, mainly in the rotor yoke and permanent magnets. One of the conditions for obtaining high values of continuous power of the motor is the reduction of these losses. This paper presents selected design methods for limiting the value of rotor losses with simultaneous consideration of their influence on other motor parameters. The analysis was carried out for a PMSM motor with an external rotor weighting approx. 10 kg and a maximum power of 50 kW at a rotational speed of 4 800 rpm.

Key words: fractional slot motors, high power density motors, rotor losses

1. Introduction

High power density motors (2–4 kW/kg continuous power) have been of particular interest in recent years. At the same time, there is a lot of interest and market need for this type of machine [1–3]. It results mainly from the implementation of electric drives in applications for which the mass of the drive is of great importance or even constitutes a key access criterion, e.g., in aviation, the nautical industry or also in selected automotive applications. Fractional slot PMSM motors allow for obtaining high power density factors, mainly due to the possibility of producing



© 2022. The Author(s). This is an open-access article distributed under the terms of the Creative Commons Attribution-NonCommercial-NoDerivatives License (CC BY-NC-ND 4.0, <https://creativecommons.org/licenses/by-nc-nd/4.0/>), which permits use, distribution, and reproduction in any medium, provided that the Article is properly cited, the use is non-commercial, and no modifications or adaptations are made.

machines with a large number of magnetic poles $2p$ and a relatively small number of stator slots Q_s . In addition, these types of motors, compared to other machines, are characterized by a shorter length of end connections, thus lower weight and losses in copper, lower cogging torque and lower torque ripple. Unfortunately, they are also marked by a quite significant disadvantage, i.e., a greater content and amplitude of higher harmonics and subharmonics in the distribution of the MMF (Magnetomotive Force) [4–9]. When operating with high frequencies of the supply voltage, high magnetic saturation and a high degree of current load, it causes losses in the rotor elements, mainly in the rotor yoke and permanent magnets. The value of these losses may cause excessive heating of the rotor elements and even lead to demagnetization of permanent magnets [10]. Thus, one of the main conditions for obtaining appropriate values of continuous motor power is effective reduction of losses in the rotor.

The aim of this study is to present selected design methods of reducing rotor losses simultaneously, with particular emphasis on their impact on key operating parameters and technological aspects of their possible introduction. This is very important because it often happens that the methods of limiting the negative impact of a given factor suggested in the literature cause a significant deterioration of other key parameters or require very costly financial outlays related to the significant complexity of the technological process. These are then methods that have no practical application, so they become useless, therefore. In this paper, for the presented methods of reducing rotor losses, both their influence on the operating parameters of the motor is given and the degree of possible complexity of the technological process or potential financial outlays because of their introduction was estimated.

The phenomenon of rotor losses is generally known and quite widely described in the literature [5–10], as well as the methods allowing to limit their negative impact [5, 6, 11–14]. However, the authors of the above papers present the problem in their publications basically from the theoretical point of view, without considering the specific application in high power density motor as the final function of the goal. These types of motors operate under operating conditions incomparable to other machines. At the same time, there are high supply frequencies (more than 800 Hz), high current loads (12–15 A/mm²) and high saturation induction (approx. 2–2.2 T), which has a direct impact on both the obtained motor parameters and the high value of rotor losses. In the authors' opinion, it is very important to analyze the methods allowing to reduce rotor losses, considering the specificity of operation of motors with high power density, which has been presented in this paper.

In the literature, individual methods of reducing rotor losses are usually presented separately, for example, the problem of the correct selection of slot-pole combination [4, 11], segmentation of permanent magnets [12, 13, 15, 16]. Such an approach, without taking into account the whole spectrum of issues also including a problem of a technological nature, may lead to conclusions that are not practically applicable in the context of high power density motors. In this paper, in a collective and comprehensive way the most important, in the authors' opinion, design methods allowing one to reduce rotor losses at the stage of designing a high-power density motor are presented.

The methods presented in this paper constitute an optimization process as a whole, in the sense that they ultimately lead to the achievement of the assumed objective function, which is the minimization of rotor losses with the simultaneous maximization of the motor power obtained. However, the presented results are not a consequence of the application of the optimization algorithm, as in works [17–19].

The analysis was performed using 2-dimensional FEM models. The subject of the analysis is a PMSM motor with an external rotor weighing approx. 10 kg and an outer diameter of 200 mm, with a maximum power of 50 kW at a speed of 4800 rpm. In the selected scope, the analysis was also presented in relation to the results of laboratory tests carried out on the physical model of the motor.

2. Motor calculation model

The subject of the analysis is a high-pole, fractional slot, PMSM motor with an external rotor. Figure 1 shows an example of a motor model with the slot – pole combination $2p = 20$, $Q_s = 30$. The computational analysis was performed using the 2D FEM method, therefore the end effects were not considered. ANSYS electromagnetic software was used for the calculations.

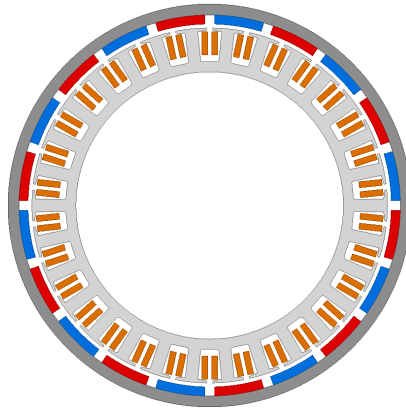


Fig. 1. Model of 20-pole, 30-slots motor

The mathematical model of the motor is described by Eqs. (1)–(5) [20]:

$$V_{sd} = R_s \cdot i_{sd} + \frac{d\Psi_{sd}}{dt} - \omega \cdot \Psi_{sq}, \quad (1)$$

$$V_{sq} = R_s \cdot i_{sq} + \frac{d\Psi_{sq}}{dt} + \omega \cdot \Psi_{sd}, \quad (2)$$

$$\Psi_{sd} = (L_1 + L_m) \cdot i_{sd} + \Psi_{PM}, \quad (3)$$

$$\Psi_{sq} = (L_1 + L_m) \cdot i_{sq}, \quad (4)$$

$$T_\Psi = p \cdot \Psi_{PM} \cdot i_{sq}, \quad (5)$$

where: V_{sd} is the phase voltage in the d -axis, V_{sq} is the phase voltage in the q -axis, i_{sd} is the phase current in the d -axis, i_{sq} is the phase current in the q -axis, Ψ_{sd} is the flux in the d -axis, Ψ_{sq} is the flux in the q -axis, Ψ_{PM} is the permanent magnet flux, R_s is the phase resistance of the stator winding, L_1 is the leakage inductance, L_m is the magnetizing inductance, ω is the electrical angular speed, T_Ψ is the electromagnetic torque, p is the number of pole pairs.

Table 1 shows the common data and assumptions made for the computational models analyzed in this article. For all analyzed models, a liquid cooling system was assumed and the permissible rated current density in the winding would be $J = 15 \text{ A/mm}^2$.

Table 1. Basic data for the FEM models of motor

Parameter	
DC supply voltage (V)	400
Max. rotational speed (rpm/min)	4 800
Rated current density (A/mm^2)	15
Flux weakening	none
Outer diameter of rotor core (mm)	200
Length of core (mm)	50
Number of phases	3
Winding temperature ($^{\circ}\text{C}$)	120
PM temperature ($^{\circ}\text{C}$)	80
Stator core material type	NO27, 0.27 mm
Type of magnets	N45SH

The comparison of the influence of the given methods presented in this paper on the parameters of the motor always refers to the obtained shaft torque T_{shaft} or shaft power P_{shaft} , not the electromagnetic torque T_{Ψ} or electromagnetic power P_{Ψ} . It is very important because it should be considered that the electromagnetic torque/power is ultimately reduced by the losses in the stator core ΔP_{Fes} , mechanical losses ΔP_{mech} and the losses in the rotor ΔP_{Tr} – Eqs. (6)–(8). Therefore, when comparing solutions based on electromagnetic torque/power, erroneous conclusions can be drawn when the share of losses in the rotor and stator core in relation to the total losses is large [21].

$$P_{\text{shaft}} = P_{\Psi} - \Delta P_{\text{Fes}} - \Delta P_{\text{Tr}} - \Delta P_{\text{mech}}, \quad (6)$$

$$T_{\text{shaft}} = \frac{30}{\pi \cdot n} \cdot P_{\text{shaft}}, \quad (7)$$

$$P_{\Psi} = \frac{2 \cdot \pi \cdot n}{60} \cdot T_{\Psi}. \quad (8)$$

3. Rotor losses

For the PMSM motor, using the developed calculation model, the total value of losses in the rotor ΔP_{Tr} was calculated as the sum of losses in the permanent magnets ΔP_{PM} and rotor yoke ΔP_{Yr} .

$$\Delta P_{\text{Tr}} = \Delta P_{\text{PM}} + \Delta P_{\text{Yr}}. \quad (9)$$

It is known that the dominant losses in rotor elements are eddy current losses P_c [22]. The eddy current losses strongly depend on the resistivity of the material of a given element. The conductivity of NdFeB permanent magnets is approx. 0.625 MS/m, while the conductivity of the materials used in the rotor yoke is approx. 1.95 MS/m, therefore the eddy current losses cannot be ignored.

The eddy current losses ΔP_c in solid material can be calculated from the expression [22]:

$$\Delta P_c = \frac{\sigma \cdot b^2}{12 \cdot f \cdot \rho} \cdot \frac{1}{T} \cdot \int_0^T \left(\frac{dB}{dt} \right)^2 dt, \quad (10)$$

where: σ is the electrical conductivity, b is the material thickness, f is the frequency, ρ is the mass density, B is the flux density, T is the period.

For the laminated core, power losses in rotor elements ΔP_{Fer} can be calculated according to expression (11), where P_h is the component of hysteresis losses, P_c is the component of eddy current losses, P_e is the component of excess losses, K_h is the hysteresis loss coefficient, K_c is the eddy current loss coefficient, K_e is the excess losses coefficient.

$$\Delta P_{\text{Fer}} = P_h + P_c + P_e, \quad (11)$$

$$P_h = K_h \cdot B^2 \cdot f, \quad (12)$$

$$P_c = K_c \cdot (B \cdot f)^2, \quad (13)$$

$$P_e = K_e \cdot (B \cdot f)^{1.5}. \quad (14)$$

Eddy current loss coefficient from Formula (13) is calculated as:

$$K_c = \pi^2 \cdot \sigma \cdot \frac{b^2}{6}. \quad (15)$$

4. The number of magnetic poles

The choice of the number of magnetic poles of a motor depends on many factors and cannot be made with the sole aim of reducing rotor losses. First, the maximum possible frequency of the power supply of the envisaged power electronic system and the required range of motor speed regulation should be considered. It is known that increasing the number of magnetic poles in the motor allows one to obtain higher torque values and reduce the mass of the electromagnetic circuit, while also increasing the frequency and thus power losses. Table 2 shows a comparison of 3 solution variants, all with the same number of slots per pole and phase $q = 0.5$ (identical MMF force distribution), but with a different number of magnetic poles. The solution $q = 0.5$ was chosen due to the lack of subharmonics and the relatively small content of higher harmonics in the MMF magnetomotive force. The FEM calculations assumed a solid rotor core and no permanent magnet segmentation.

Figure 2 shows a comparison of total losses for the analyzed variants of the solution with a different number of magnetic poles.

Table 2. Comparison of motor parameters for variants $q = 0.5$ with different number of magnetic poles ($J = 15 \text{ A/mm}^2$)

	f	ΔP_{Fes}	ΔP_{Yr}	ΔP_{PM}	P_{shaft}	T_{shaft}	η
	Hz	W	W	W	kW	Nm	%
$2p = 12, Q_s = 18$	480	387	978	1 164	25.5	50.8	85.0%
$2p = 10, Q_s = 27$	720	1 117	260	342	31.4	62.5	89.8%
$2p = 20, Q_s = 30$	800	1 263	191	273	32.1	63.9	90.0%

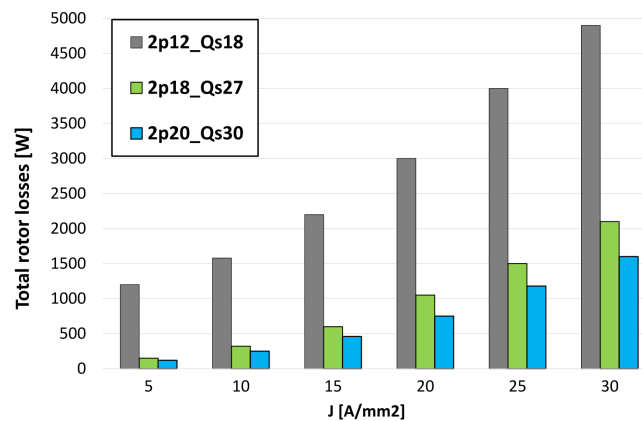


Fig. 2. Total rotor losses as a function of the current load for solutions with $q = 0.5$ with a different number of magnetic poles ($n = 4\ 800 \text{ rpm}$)

Analyzing the data from Table 2 and Fig. 2, the increase in the number of magnetic poles reduced the losses in the rotor even by approx. 80%, and at the same time the shaft torque and shaft power increased by approx. 25%. One of the reasons for this is a reduction of the magnet's pole pitch with an increase in the number of magnetic poles, and thus a reduction in the volume of individual magnets. Additionally, it should be noted that despite the identical dimensions of the solid rotor core for each variant, along with the increase in the number of magnetic poles, the losses in the yoke also significantly decrease.

Thus, the increase in the number of magnetic poles contributed to a significant improvement in the parameters of the motor, despite the increase in the supply frequency. The disadvantageous effect, however, is the increase in losses in the stator core, mainly due to an increase in the supply frequency. These losses increased 3 times, so it should be considered whether the selected cooling system is able to dissipate this value of losses. Two more things should be noted at this point. First, stator losses are easier to dissipate than rotor losses due to better cooling conditions. The second point is that despite the 3-times increase in the losses in the stator core, the overall efficiency η of the motor has increased by as much as 5% compared to the solution with a large number of rotor losses.

With reference to the above analysis, a motor with the number of magnetic poles $2p = 20$ was selected as the target variant.

5. Slot/pole combinations

The previous chapter shows the influence of the selection of the number of magnetic poles on the rotor losses and the motor operating parameters. This chapter presents the problem of the correct selection of the number of slot/pole combinations. It is crucial and of prime importance in limiting the value of eddy current losses in the rotor. The fractional slot motor is characterized by the content of subharmonics and higher harmonics in the MMF distribution, which is one of the main causes of losses in the rotor elements. Their content can be limited by the appropriate selection of slot/pole combinations. This issue was presented in detail, in the work [21].

For the analysis, a motor model with the number of magnetic poles $p = 20$ and a solid rotor core was adopted and no permanent magnet segmentation assumed. Solutions characterized by a high winding factor k_w were selected (Table 3).

Table 3. Basic winding parameters for the analyzed slot/pole combinations

$2p$	Q_s	q	k_w
20	18	0.3	0.945
20	21	0.35	0.953
20	24	0.4	0.933
20	30	0.5	0.866

Table 4 and Fig. 3 present a comparison of the obtained parameters and losses for the analyzed variants. The obtained results show how important it is to correctly select the slot-pole combination for the value of rotor losses. For the rated current density of $J = 15 \text{ A/mm}^2$, the difference in the value of losses in the rotor between the extreme solutions is 6200 W and it grows exponentially with a further increase in the current load. In addition, it should be noted that the solution $p = 20$, $Q_s = 18$ with a much higher value of the winding factor than the solution $2p = 20$, $Q_s = 30$, and therefore proportionally to these higher values of the electromagnetic torque, ultimately has a much lower shaft torque and shaft power, as part of the supply current covers the increased rotor losses. Therefore, when comparing the presented solutions, it should

Table 4. Comparison of motor parameters for variants $p = 20$ with different slot/pole combinations ($J = 15 \text{ A/mm}^2$)

	f	ΔP_{Fes}	ΔP_{Yr}	ΔP_{PM}	P_{shaft}	T_{shaft}	η
	Hz	W	W	W	kW	Nm	%
$2p = 20$, $Q_s = 18$	800	2 005	4 693	2 015	26.5	52.6	71.0%
$2p = 20$, $Q_s = 21$	800	1 480	1 706	1 214	32.9	65.4	83.5%
$2p = 20$, $Q_s = 24$	800	923	635	567	33.2	66.0	89.0%
$2p = 20$, $Q_s = 30$	800	1 263	191	273	32.1	63.9	90.0%

be stated that the solution $p = 20$, $Q_s = 30$ with the coefficient $q = 0.5$ is characterized by both high operating parameters of the motor and the lowest value of losses in the rotor despite the lowest value of the winding factor k_w . Moreover, according to [21], solutions with the number of slots Q_s lower than the number of magnetic poles $2p$ are characterized by the highest values of losses in the rotor and should be avoided, especially when operating with high values of supply frequency and high values of current loads.

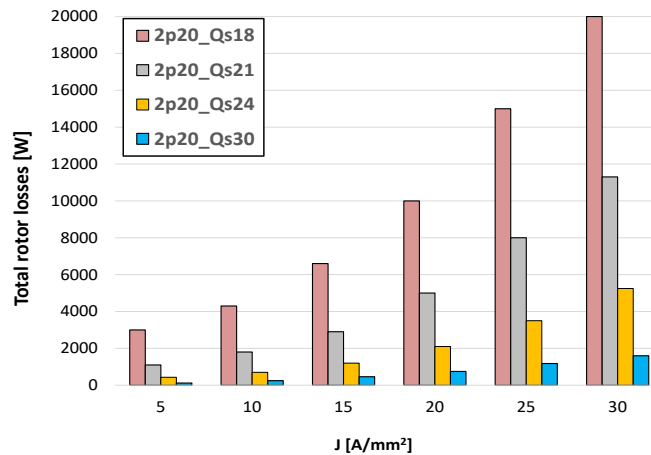


Fig. 3. Total rotor losses as a function of current load for different slot/pole combinations ($2p = 20$, $n = 4800$ rpm)

The above analysis shows the legitimacy of using two of the analyzed solutions, the variant $2p = 20$, $Q_s = 24$ and the variant $p = 20$, $Q_s = 30$. Finally, to make the physical model, the variant $p = 20$, $Q_s = 24$ was selected due to the higher values of shaft power and shaft torque, at the same time taking into account the possibility of effective dissipation of increased rotor losses.

6. Segmentation of permanent magnets

The segmentation of permanent magnets is a known and described in the literature [12, 13, 15, 16, 23] method of reducing losses in magnets. This applies to both circumferential and axial segmentation. In the case of high-pole motors with high power density, however, the following practical points should be considered:

- the width of the permanent magnet is already small, therefore additional circumferential segmentation significantly complicates the technological process of gluing the magnets and thus increases the cost of producing the rotor. Therefore, it is a rather deprecated method, unless it is necessary to use magnets with unacceptable dimensions from a technological point of view,
- axial segmentation also reduces permanent magnet losses and allows for a skew in the rotor that minimizes cogging torque. Therefore, it is a recommended method, considering the

number of segments so that the dimensions of the magnet are acceptable in the technological process.

Ultimately, based on the results of the work described in the literature, a 4-fold axial segmentation was used in the physical model of the motor.

7. Rotor core material type

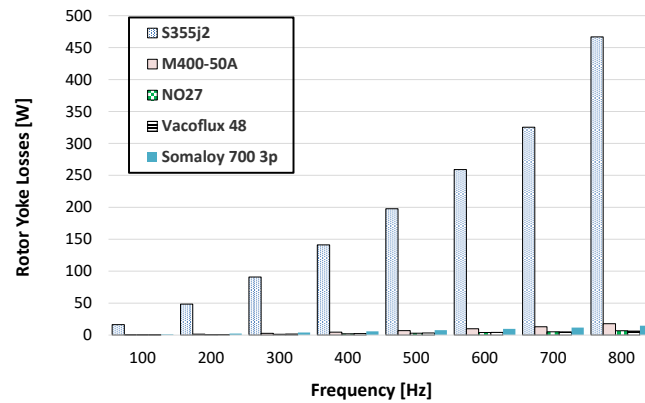
According to Eq. (10), the eddy current losses in the rotor elements are strongly dependent on the material properties. The parameters of the motor also closely depend on the materials used in the electromagnetic circuit [24]. For this analysis, the motor model $p = 20$, $Q_s = 24$ was used. The influence of the rotor yoke material properties on the rotor losses and the motor operating parameters was analyzed. The analysis was performed for the solid rotor core (steel S355j2), the laminated core (M400-50A, NO27, Vacoflux48) and SMC (Soft Magnetic Composite) rotors (Somaloy 700 3p). In the case of a high-power density motor with an external rotor, the production of the solid rotor core simplifies the technological process and eliminates the need to use additional fastening elements. These elements increase both the dimensions and weight of the motor, and thus ultimately lower the power density factor. Table 5 presents the basic properties of the analyzed material and the loss coefficients K_h , K_c , and K_e used in Eqs. (11)–(14).

Table 5. Material properties which analyzed in the rotor

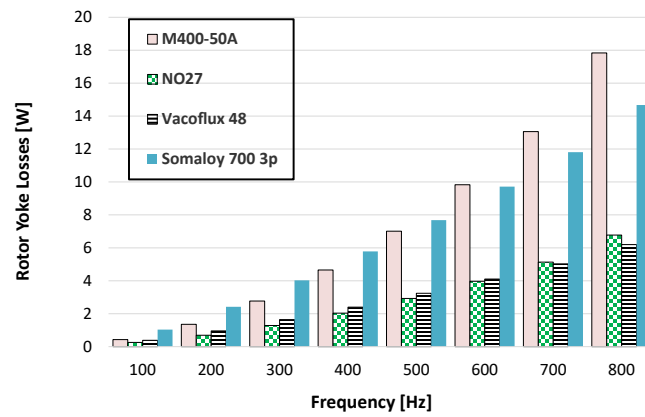
Type of material in rotor yoke	Conductivity	Mass density	K_h	K_c	K_e
	MS/m	kg/m ³	W/m ³		
S355j2	1.95	7 700	–	–	–
M400-50A	1.95	7 700	163.2	1.28	0
NO27	1.7	7 600	115.6	0.34	0.72
Vacoflux48	2.27	8 120	46.4	0.014	3.67
Somaloy 700 3p	0.005	7 500	579.1	0	14.52

Figure 4 shows a comparison of losses in the rotor yoke for the analyzed cases of the rated current load as a function of the frequency of the supply voltage. For clarity of the results, the comparison is shown in two graphs with and without the solid rotor core variant.

Table 6 presents a comparison of the obtained parameters and individual losses for the analyzed variants. The presented results show that the use of a laminated rotor yoke significantly reduces the losses in the yoke, regardless of the type of sheet used. In addition, a slight improvement in the shaft torque and shaft power parameters is also observed due to the reduction of rotor losses. At this point, however, it should be added that the mere fact of significantly greater losses in the yoke for the solid rotor core does not eliminate this solution definitively. The use of a solid core in a motor with an external rotor significantly simplifies the structure and technological process, as it does not require additional supporting elements, as is the case with a laminated core. For this



(a)



(b)

Fig. 4. Comparison of losses in the rotor yoke for different yoke material for the rated current load as a function of the supply frequency: comparison of the solid core and laminated cores (a); comparison of laminated cores only (b)

Table 6. Comparison of motor parameters with different materials of rotor yoke for $n = 4800$ rpm, $J = 15$ A/mm²

	f	ΔP_{Fes}	ΔP_{Yr}	ΔP_{PM}	P_{shaft}	T_{shaft}	η
	Hz	W	W	W	kW	Nm	%
S355j2	800	923	635	567	33.2	66.0	89.0%
M400-50A	800	980	18	513	33.8	67.3	89.8%
NO27	800	962	7	536	33.9	67.4	89.8%
Vacoflux48	800	950	6	631	34.0	67.6	89.8%
Somaloy 700 3p	800	975	15	506	33.6	66.8	89.7%

reason, after the thermal analysis performed, it was decided that the first physical model of the motor would be made with a solid rotor core. Nevertheless, the above analysis shows the potential for reducing losses in the event of thermal problems on the test bench.

8. Slot opening width

Another important design parameter that has a significant impact on the rotor losses' value is the stator slot opening width b_{s0} . A large slot opening causes additional pulsations in the wave of magnetic induction in the air gap, while too small size increases the value of slot leakage flux and causes additional technological problems during winding. The analysis of the influence of the slot opening width on the rotor losses and the operating parameters of the motor was carried out for several variants differing in the number of magnetic poles:

- a) $2p = 18, Q_s = 27, q = 0.5,$
- b) $p = 20, Q_s = 30, q = 0.5,$
- c) $2p = 24, Q_s = 36, q = 0.5,$
- d) $2p = 40, Q_s = 45, q = 0.375.$

For each of the variants, the analysis was carried out from the minimal to the full opening of the stator slot. The computational models assume a laminated rotor core, therefore almost the entire value of rotor losses are losses in permanent magnets.

Figure 5 shows the characteristics of total rotor losses as a function of the slot opening width for various slot/pole combinations. Figure 6 shows a comparison of the influence of the slot opening width on the shaft of the motor.

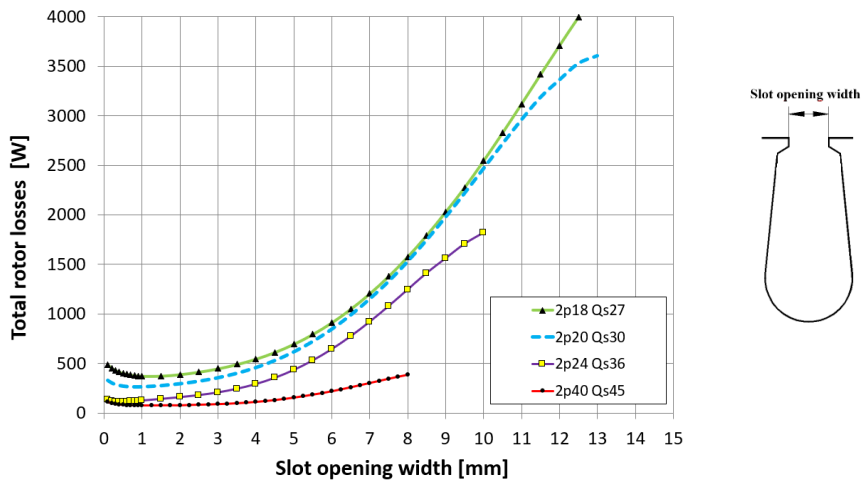


Fig. 5. Total rotor losses as a function of the slot opening width for different slot/pole combinations ($f = 800 \text{ Hz}, J = 15 \text{ A/mm}^2$)

When analysing Figs. 5 and 6, the slot opening width has a significant impact on the value of losses in the rotor and the torque obtained on the motor shaft. The influence on the rotor

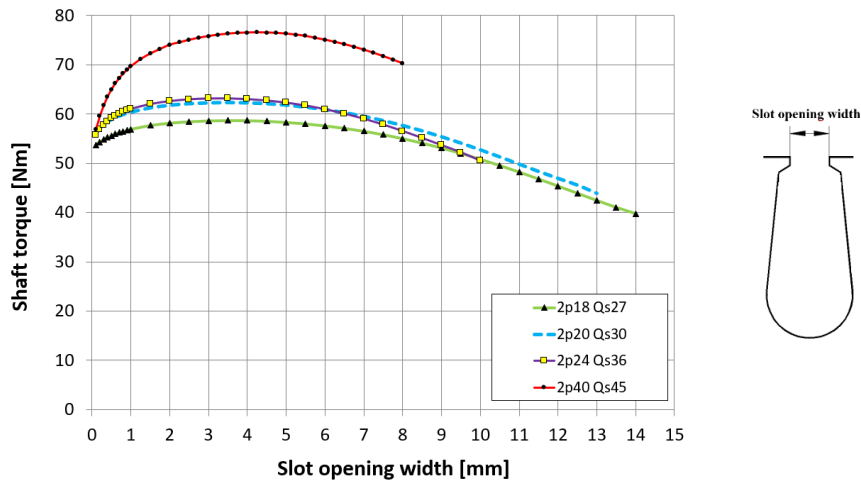


Fig. 6. Shaft torque as a function of the slot opening width for different slot/pole combinations ($f = 800 \text{ Hz}$, $J = 15 \text{ A/mm}^2$)

losses, however, is different depending on the number of magnetic poles of the motor, and as the number of magnetic poles increases, the difference between the minimum and maximum value of rotor losses decreases. The graphs show the most favourable slot opening widths for which the minimum value of rotor losses and at the same time large values of shaft torque (around the maximum) are obtained. Finally, the slot opening width in the physical model of the motor was $b_{s0} = 1.8 \text{ mm}$, because the technological aspects of the winding process were also considered.

9. Physical model and lab tests

Based on the analysis presented in this paper, the final motor solution was designed, and a FEM simulation was performed for it. Then, the physical model of the motor was developed, the parameters of which were verified on the test stand. The purpose of the methods described in the paper was to develop a solution allowing one to obtain a high value of the continuous power density factor, inseparably linked with the necessity to reduce rotor losses. Figure 7(a) shows the model of the motor on the test stand. Figure 7(b) shows the scheme of the measurement system.

The basic data of the motor model, considering the results of the analysis presented in the paper, are presented in Table 7.

The test results for the rated load current as a function of rotational speed are presented in Table 8. The calculations assumed that the rated current density would be approx. 15 A/mm^2 . During the tests it turned out that it is slightly lower, $J = 13.7 \text{ A/mm}^2$. For such a current load, the rotor and stator temperatures were at their limit values. The rotor temperature was measured with the Flir E300 thermal imaging camera, while the stator winding temperature was measured with the installed Pt100 sensors.

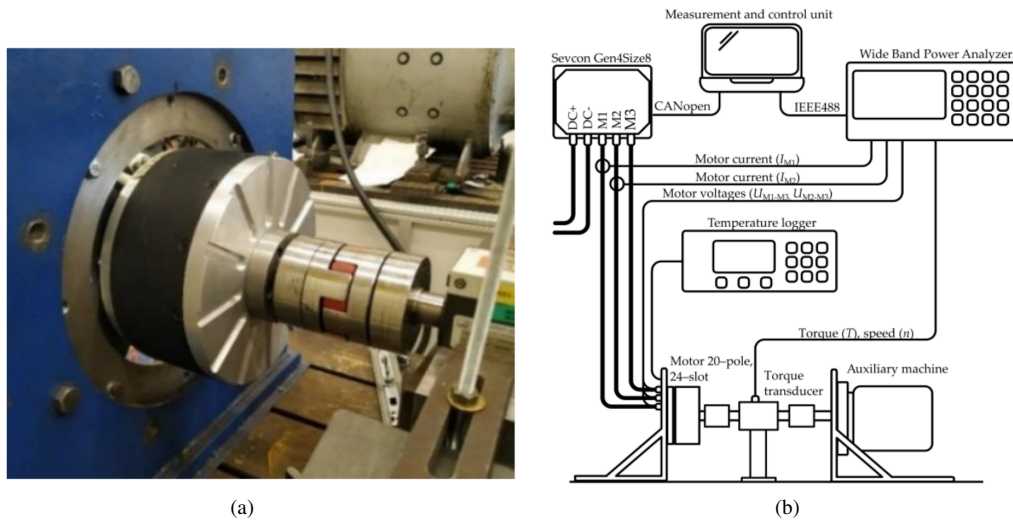


Fig. 7. Physical model of the motor (a); scheme of the measuring system (b) [12]

Table 7. Data of the physical model of the motor

Parameter	
DC supply voltage (V)	400
Max. rotational speed (rpm/min)	4 800
Outer diameter (mm)	200
Length of motor (mm)	105
Stator core material type	NO27, 0.27 mm
Type of magnets	N45SH
Motor weight (kg)	10.5
Number of magnetic poles	20
Slot – pole combination	20/24
Circumferential segmentation of PM	none
Axial segmentation of PM	4
Rotor core material type	S355j2
Slot opening width (mm)	1.8

Figure 8 shows a comparison of the calculation results with the results of laboratory tests for the shaft torque as a function of the current load for the maximum rotational speed $n = 4\,800$ rpm.

Table 8. The results of tests bench of a motor for the rated current I_N

n	f	P_{shaft}	T_{shaft}	η	T_{rotor}	T_{stator}
rpm	Hz	kW	Nm	%	°C	°C
600	100	3.8	60.5	79.3	60	95
1 200	200	7.4	58.9	84.9	83	105
1 800	300	11.0	58.4	87.2	100	111
2 400	400	14.5	57.7	89.1	101	116
3 000	500	17.3	55.1	89.3	107	120
3 600	600	20.0	53.1	89.5	116	123
4 200	700	22.8	51.8	90.5	121	126
4 800	800	25.4	50.5	89.9	130	129

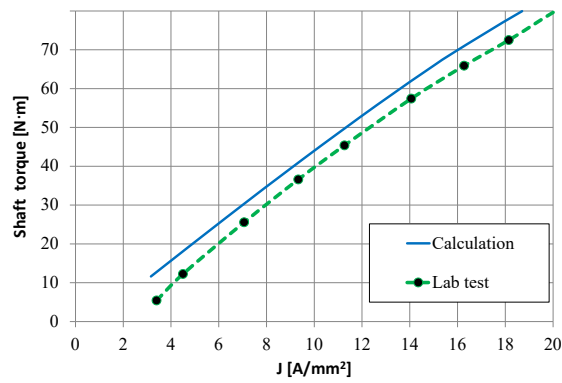


Fig. 8. Comparison of calculations and lab tests for shaft torque for 20 – pole, 24 – slot motor ($n = 4\,800$ rpm)

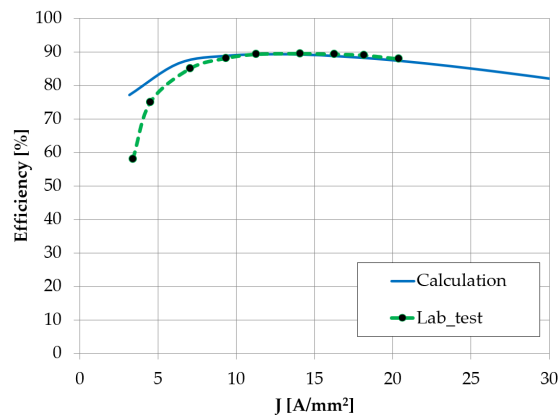


Fig. 9. Comparison of calculations and lab tests for efficiency for 20 – pole, 24 – slot motor ($n = 4\,800$ rpm)

Figure 9 shows a comparison of the calculation results with the results of laboratory tests of efficiency as a function of the current load for the maximum rotational speed $n = 4800$ rpm. A relatively good convergence of results can be stated.

10. Conclusions

Rotor losses in the case of fractional slot motors are not negligible and must be considered at the design stage. This paper presents selected design methods limiting the value of rotor losses in fractional slot motors with high power density. At the same time, attention was focused on the impact of individual methods on the key operating parameters of the motor and the technological aspects of their possible introduction. For motors with high power density, it is primarily the value of the torque on the motor shaft. Five key aspects were noted and discussed: the correct selection of the number of magnetic poles, the selection of the appropriate slot - pole combination, permanent magnet segmentation, the type of materials used in the rotor yoke and the slot opening width. Each of these issues, if not considered at the design stage, may result in excessive losses in the rotor, resulting in exceeding the allowable temperatures.

On the basis of the presented methods, a physical model of the motor was designed and laboratory verification was performed. The obtained continuous power factor of the motor is 2.4 kW/kg, so the purpose of the work was achieved. The design of the motor's electromagnetic circuit with appropriate consideration of the methods presented in the paper allows one to reduce rotor losses and thus obtain high values of continuous power.

Acknowledgements

This paper was supported and financed by the NCBR, project LIDER/31/0169/L-12/20/NCBR/2021.

References

- [1] Ramesh P., Lenin C.N., *High Power Density Electrical Machines for Electric Vehicles – Comprehensive Review Based on Material Technology*, IEEE Transaction on Magnetics, vol. 55, no. 11 (2019), DOI: [10.1109/TMAG.2019.2929145](https://doi.org/10.1109/TMAG.2019.2929145).
- [2] Sudha B., Anusha V., Sachin S., *A review: High power density motors for electric vehicles*, Journal of Physics: Conference Series, vol. 1706, pp. 1–8 (2020), DOI: [10.1088/1742-6596/1706/1/012057](https://doi.org/10.1088/1742-6596/1706/1/012057).
- [3] Wolnik T., Dukalski P., Będkowski B., Jarek T., *Selected aspects of designing motor for direct vehicle wheel drive*, Przegląd Elektrotechniczny (Electrical Review), vol. 96, pp. 150–153 (2020), DOI: [10.15199/48.2020.04.31](https://doi.org/10.15199/48.2020.04.31).
- [4] Bianchi N., Bolognani S., Pre M.D., *Magnetic loading of fractional slot three phase PM motors with non overlapped coils*, In Proceedings of the IEEE Conference Record of the 2006 IEEE Industry Applications Conference Forty-First IAS Annual Meeting, Tampa, USA, pp. 35–43 (2006), DOI: [10.1109/IAS.2006.256517](https://doi.org/10.1109/IAS.2006.256517).
- [5] Bianchi N., Bolognani S., Fomasiero E., *A General Approach to Determine the Rotor Losses in Three-Phase Fractional-Slot PM Machines*, IEEE International Electric Machines and Drives Conference – Antalya, Turkey, pp. 634–641 (2007), DOI: [10.1109/IEMDC.2007.382741](https://doi.org/10.1109/IEMDC.2007.382741).

- [6] Ishak D., Zhu Z.Q., Howe D., *Eddy-current loss in the rotor magnets of permanent-magnet brushless machines having a fractional number of slots per pole*, IEEE Transaction on Magnetics, vol. 41, pp. 2462–2469 (2005), DOI: [10.1109/TMAG.2005.854337](https://doi.org/10.1109/TMAG.2005.854337).
- [7] Atallah K., Howe D., Mellor P.H., Stone D.A., *Rotor loss in permanent-magnet brushless AC machines*, IEEE Transaction on Industry Applications, vol. 36, pp. 1612–1618 (2000), DOI: [10.1109/28.887213](https://doi.org/10.1109/28.887213).
- [8] Yu X., Guoli L., Zhe Q., Qiubo Y., Zhenggen Z., *Research on rotor magnet loss in fractional-slot concentrated-windings permanent magnet motor*, 2016 IEEE 11th Conference on Industrial Electronics and Applications (ICIEA), Hefei, China, pp. 1616–1620 (2016).
- [9] Aslan B., Semail E., Legranger J., *General Analytical Model of Magnet Average Eddy-Current Volume Losses for Comparison of Multiphase PM Machines With Concentrated Winding*, IEEE Transactions on Energy Conversion, vol. 29, pp. 72–83 (2014), DOI: [10.1109/TEC.2013.2292797](https://doi.org/10.1109/TEC.2013.2292797).
- [10] Wolnik T., Styskala V., Hrbac R., Lyaschenko A.M., *The Problem of Rotor Eddy-Current Losses in A Permanent Magnet Motor with High Power Density*, In Proceedings of the International Conference on Intelligent Information Technologies for Industry IITI2021, Sochi, Russia, pp. 501–512 (2021), DOI: [10.1007/978-3-030-87178-9_50](https://doi.org/10.1007/978-3-030-87178-9_50).
- [11] Aslan B., Semail E., Korecki J., Legranger J., *Slot/pole combinations choice for concentrated multiphase machines dedicated to mild-hybrid applications*, IECON 2011 – 37th Annual Conference of the IEEE Industrial Electronics Society, pp. 3698–3703 (2011).
- [12] Ede J., Atallah K., Jewell G.W., Wang J.B., Howe D., *Effect of Axial Segmentation of Permanent Magnets on Rotor Loss in Modular Permanent-Magnet Brushless Machines*, IEEE Transactions on Industry Applications, vol. 43, pp. 1207–1213 (2007), DOI: [10.1109/TIA.2007.904397](https://doi.org/10.1109/TIA.2007.904397).
- [13] Wan-Ying Huang, Bettayeb A., Kaczmarek R., Vannier J.-C., *Optimization of Magnet Segmentation for Reduction of Eddy-Current Losses in Permanent Magnet Synchronous Machine*, IEEE Transactions on Energy Conversion, vol. 25, pp. 381–387 (2010), DOI: [10.1109/TEC.2009.2036250](https://doi.org/10.1109/TEC.2009.2036250).
- [14] Młot A., Kowol M., Kołodziej J., Lechowicz A., Skrobotowicz P., *Analysis of IPM motor parameters in an 80-kW traction motor*, Archives of Electrical Engineering, vol. 69, no. 2, pp. 467–481 (2020), DOI: [10.24425/aee.2020.133038](https://doi.org/10.24425/aee.2020.133038).
- [15] Wills D.A., Kamper M.J., *Reducing PM eddy current rotor losses by partial magnet and rotor yoke segmentation*, IEEE 2010 XIX International Conference on Electrical Machines (ICEM), Rome, Italy (2010).
- [16] Yamazaki K., Shina M., Kanou Y., Miwa M., Hagiwara J., *Effect of Eddy Current Loss Reduction by Segmentation of Magnets in Synchronous Motors: Difference Between Interior and Surface Types*, IEEE Transactions on Magnetics, vol. 45, pp. 4756–4759 (2009), DOI: [10.1109/TMAG.2009.2024159](https://doi.org/10.1109/TMAG.2009.2024159).
- [17] Sun X., Shi Z., Guo Y., Zhu J., *Multi-Objective Design Optimization of an IPMSM Based on Multilevel Strategy*, IEEE Transactions on Industrial Electronics, vol. 68, pp. 139–148 (2021), DOI: [10.1109/TIE.2020.2965463](https://doi.org/10.1109/TIE.2020.2965463).
- [18] Sun X., Shi Z., Zhu J., *Multiobjective Design Optimization of an IPMSM for EVs Based on Fuzzy Method and Sequential Taguchi Method*, IEEE Transactions on Industrial Electronics, vol. 68, pp. 10592–10600 (2021), DOI: [10.1109/TIE.2020.3031534](https://doi.org/10.1109/TIE.2020.3031534).
- [19] Wolnik T., *Alternate computational method for induction disk motor based on 2D FEM model of cylindrical motor*, Archives of Electrical Engineering, vol. 69, no. 1, pp. 233–244 (2020), DOI: [10.24425/aee.2020.131770](https://doi.org/10.24425/aee.2020.131770).
- [20] Wilamowski B.M., Irwin J.D., *Power Electronics and Motor Drives*, 2nd ed.; CRC Press Taylor & Francis Group: Boca Raton, FL, USA (2011).

- [21] Wolnik T., Styskala V., Mlcak T., *Study on the Selection of the Number of Magnetic Poles and the Slot-Pole Combinations in Fractional Slot PMSM Motor with a High Power Density*, *Energies*, vol. 15, no. 1, p. 215 (2022), DOI: [10.3390/en15010215](https://doi.org/10.3390/en15010215).
- [22] Zhao N., Zhu Z.Q., Liu W., *Rotor Eddy Current Loss Calculation and Thermal Analysis of Permanent Magnet Motor and Generator*, *IEEE Transactions on Magnetics*, vol. 47, pp. 4199–4202 (2011), DOI: [10.1109/TMAG.2011.2155042](https://doi.org/10.1109/TMAG.2011.2155042).
- [23] Lee T., Kim Y., Jung S.-Y., *Reduction of permanent magnet eddy current loss in interior permanent magnet synchronous motor according to rotor design optimization*, *IEEE 2015 9th International Conference on Power Electronics and ECCE Asia, Seoul, South Korea*, pp. 1712–1717 (2015).
- [24] Przybylski M., *Calculations and measurements of torque and inductance of switched reluctance motors with laminated and composite magnetic cores*, *Archives of Electrical Engineering*, vol. 7, no. 1, pp. 125–138 (2022), DOI: [10.24425/ae.2022.140201](https://doi.org/10.24425/ae.2022.140201).